POLSKA AKADEMIA NAUK

INSTYTUT MASZYN PRZEPŁYWOWYCH

TRANSACTIONS OF THE INSTITUTE OF FLUID-FLOW MACHINERY

PRACE INSTYTUTU MASZYN PRZEPŁYWOWYCH

104

GDAŃSK 1998

THE TRANSACTIONS OF THE INSTITUTE OF FLUID-FLOW MACHINERY

exist for the publication of theoretical and experimental investigations of all aspects of the mechanics and thermodynamics of fluid-flow with special reference to fluid-flow machines

*

PRACE INSTYTUTU MASZYN PRZEPŁYWOWYCH

poświęcone są publikacjom naukowym z zakresu teorii i badań doświadczalnych w dziedzinie mechaniki i termodynamiki przepływów, ze szczególnym uwzględnieniem problematyki maszyn przepływowych

Wydanie publikacji zostało dofinansowane przez PAN ze środków DOT uzyskanych z Komitetu Badań Naukowych

EDITORIAL OFFICE – REDAKCJA

Wydawnictwo Instytutu Maszyn Przepływowych
Polskiej Akademii Nauk
ul. Gen. Józefa Fiszera 14, 80-952 Gdańsk, skr. poczt. 621,
☎ (0-58) 341-12-71 wew. 141, fax: (0-58) 341-61-44,
e-mail: esli@imppan.imp.pg.gda.pl

ISSN 0079-3205

TRANSACTIONS OF THE INSTITUTE OF FLUID-FLOW MACHINERY

No. 104, 1998, 119-127

MIROSLAV ŠŤASTNÝ[1], JIŘÍ BRICH[1], JIŘÍ POLANSKÝ[1]

Numerical simulation of the steam flow through a balanced control valve

Balanced control valves need lower lift force due to the use of a balancing valve cone. The main cone is freely suspended on the stem and that is why this type of control valves inclines to vibrations. It is necessary for this type of valves to pay special attention to the steam flow conditions and to the aerodynamic forces. The flow through the balanced valve was studied using a mathematical model and also experimentally.

Numerical calculations of the flow through a balanced valve is based on application of Navier-Stokes equations for compressible flowing medium together with $k-\varepsilon$ turbulence model. The RAMPANT code was used for calculations. The task was solved alternatively for the assumption of axially symmetrical flow and the 3D flow. The unstructured mesh with $(12-18)\cdot 10^3$ triangles was applied for axially symmetrical flow. The mesh of $160\cdot 10^3$ tetrahedral elements was used for 3D flow and the Multigrid solver was applied for getting better convergence.

The results of numerical simulation are compared with some experimental results of the balanced control valve.

1. Introduction

The balanced control valves need, due to the use of the balancing cone (1), lower lifting force. The main cone (2) is freely suspended on the stem and in the application of the so called beam control, is also the stem freely suspended on the beam – see diagrammatic arrangement on Fig. 1. Due to the free position of the main cone and of the stem, is this valve type very apt to vibrations. Special attention must be paid to the conditions of steam flow and to the aerodynamic forces. The flow through the valve shown in Fig. 1 was investigated by means of the mathematical model and also experimentally for different geometric arrangements. Attention is paid in the paper to the influences of the main and balancing cone shapes on the structure of steam flow through the control valve.

[1]ŠKODA TURBINY s.r.o., Plzeň, Czech Republic

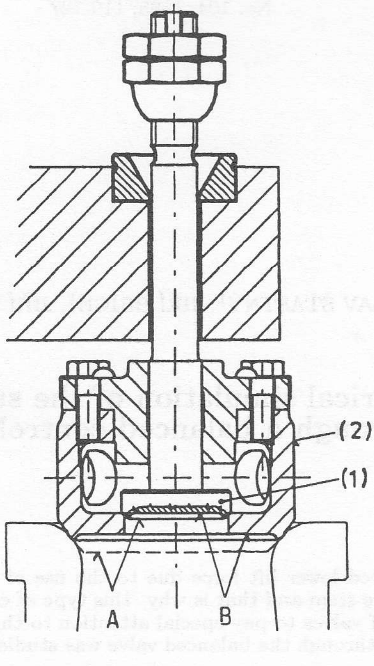

Fig. 1. Diagrammatic arrangement of the balanced control valve.

2. Computational model

The numerical solution of the flow through the balanced valve is based on the use of the Navier-Stokes equations for the compressible medium, with the $k-\varepsilon$ turbulence model reflecting the turbulence. The code RAMPANT was used for the computation. The problem was solved with the assumption of axially symmetrical flow, the 3D flow formulation and with consideration of axially symmetrical flow inlet. The triangular non-structured mesh is applied for the region of the axially symmetrical flow with the elements number $(12-18)\cdot 10^3$. For the 3D solution the mesh is used which represents the section of 1/6 valve, which contains one of six relieve openings in the main cone. The computation mesh is formed by $160\cdot 10^3$ tetrahedral elements. The example of the boundary planes of the 3D computation mesh is obvious in the Fig. 2. The solver Multigrid is used in the calculation to accelerate convergence.

The openings in the circumference of the main cone were for the axially symmetrical solution replaced by a fissure. The shapes of the main and balancing cones were investigated in 2 variants according to Fig. 1: old execution A, newer execution B.

In the next part interest is focused on two regimes of the superheated steam flow through the valve according to the Fig. 1. The first alternative presents the typical example of partially opened valve, with the relative lift of the main cone

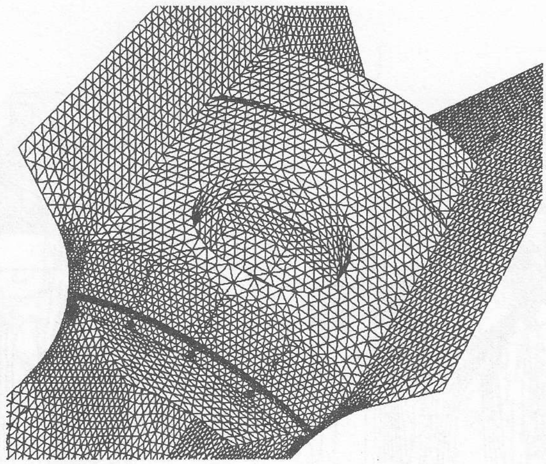

Fig. 2. 3D mesh on the computational region boundary.

$h/D = 0.04$ (h – lift of the main cone, D – smallest diffuser diameter), with the pressure ratio $\varepsilon = 0.75$. The second variant deals with the opened valve. The relative main cone lift h/D=0.6 and the pressure ration $\varepsilon = 0.96$.

3. Calculations and analysis

3.1. Partially opened valve $h/D = 0.04$

At first we present the results of the axially symmetrical flow through a partially opened valve.

The isolines of the Mach number are shown in the Fig. 3. The pressure ratio $\varepsilon = 0.75$ in the whole valve corresponds the Mach number of the isentropic flow $M_{is} = 0.68$, but the local Mach number values are considerably higher.

For the older variant of the main and balancing cone shape A, exceeding of the sonic velocity, occurs even in the channel under the main cone. The maximum Mach number $M_{max} = 1.6$ is reached in the supersonic region. Behind the supersonic region follows the shock wave and the velocity drops down below the sonic values.

For the main cone shape according to the variant **B**, velocity in the proximity of the valve seat is more favourable. The Mach number reaches the value $M_{max} = 0.9$ and the flow along the diffuser wall is more fluent. It is obvious for the variant **A** that at the bottom of the main and balancing cones there is an attached flow with the velocity gradient and this means also with the pressure gradient. The variant **B** indicates the evident stream separation at the bottom of both cones, with small differences in velocities. It corresponds to a more even

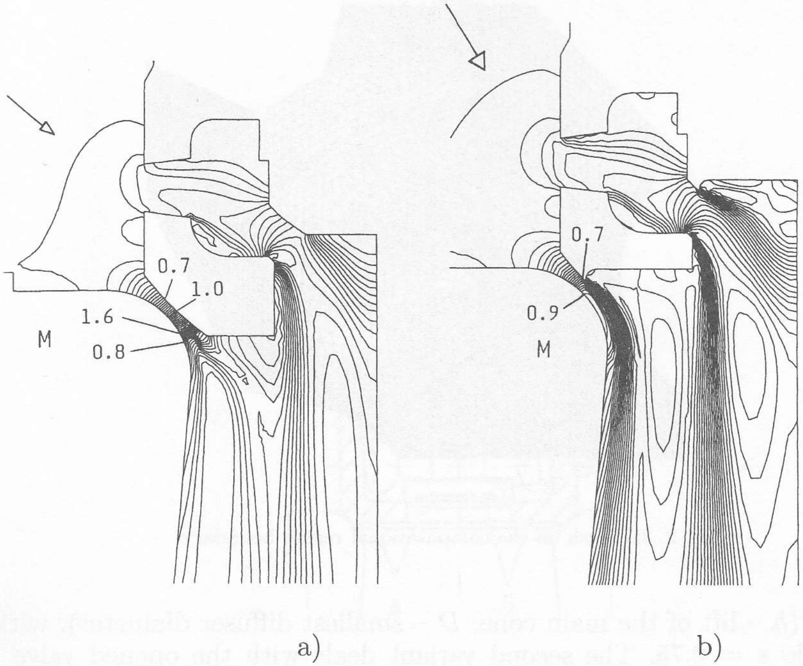

Fig. 3. Isolines of the Mach number for partially opened valve ($h/D = 0.04$) a) variant **A**, b) variant **B**.

pressure distribution. The aerodynamic force, which acts in the axis direction on the movable part of the valve is for the variant **B** lower by 6.4% compared to the variant **A**.

The flow structures are obvious from the velocity vectors distribution shown in Fig. 4. In variant **A** we observe the drop of the velocities at the diffuser wall resulting in the flow separation. In the diffuser wall proximity there is created the region filled with vortices. Steam flow is cumulated in the proximity of the diffuser axis. Flow separation does not occur at the bottom of the main and balancing cones, but the flow is close to separation. Small vortex regions are visible in the inner space of the main cone.

Structure of the flow along the main cone for the case of variant **B** is different. There is evident flow separation at the end of channel under the main cone and the flow layer has higher velocity along the diffuser wall. Between the central and the wall flow in the diffuser is the vortex region. Also at the bottom of the balancing cone the flow separation is unambiguous. The vortex regions are present also in the inner space of the main cone.

In Fig. 5 the distribution of the streamlines are shown. Main differences between the variants **A** and **B** are in the outer flow layer in the diffuser. As it was already mentioned, the variant **A** is marked by the flow concentration close to the diffuser axis. In variant **B** one part of the flow goes near to the axis and the other close to the diffuser wall. The total mass flow is increased for the variant

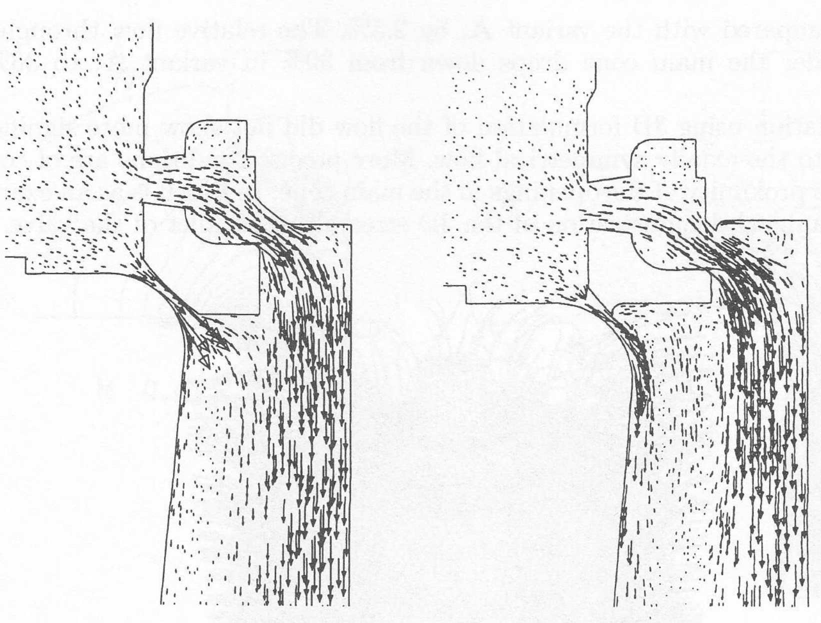

a) b)

Fig. 4. Velocity vectors for partially opened valve ($h/D = 0.04$) a) variant **A**, b) variant **B**.

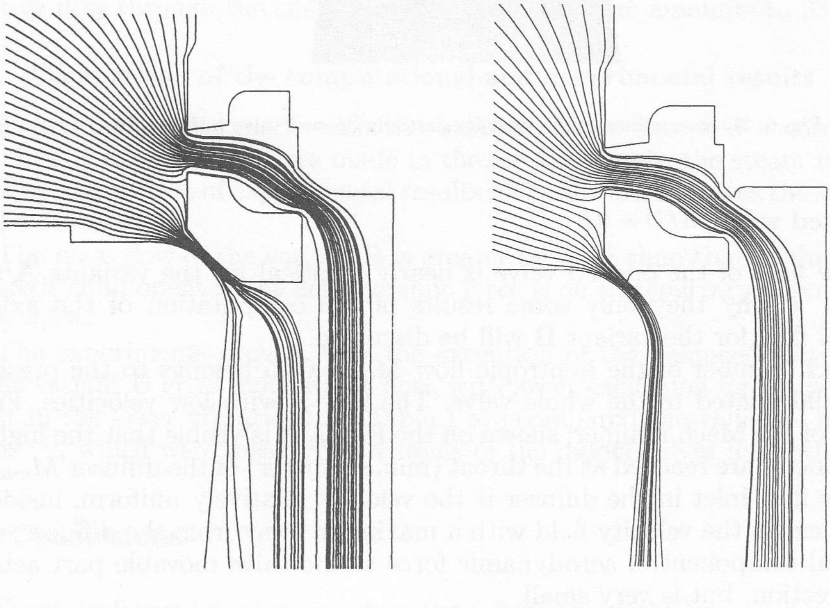

a) b)

Fig. 5. Streamline distribution for partially opened valve ($h/D = 0.04$) a) variant **A**, b) variant **B**.

B, when compared with the variant **A**, by 2.5%. The relative flow through the channel under the main cone drops down from 39% in variant **A**, to 36% in variant **B**.

Computation using 3D formulation of the flow did not show more significant differences to the axially symmetrical flow. More precise conditions are of course found in the proximity of the openings in the main cone. In Fig. 6 is as an example shown a graphical demonstration of the 3D streamlines at inlet of the valve.

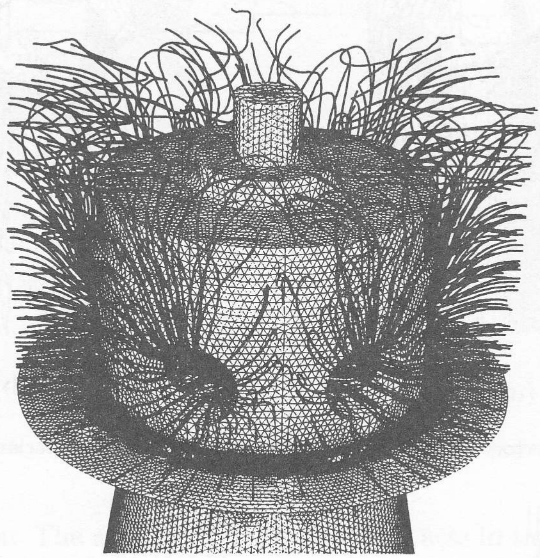

Fig. 6. 3D streamlines at the inlet for partially opened valve $h/D = 0.04$.

3.2. Opened valve, $h/D = 0.6$

The flow field of the opened valve is nearly identical for the variants **A** and **B** and that is why they only some results of the computation of the axially symmetrical flow for the variant **B** will be discussed.

The Mach number of the isentropic flow $M_{is} = 0.25$ belongs to the pressure ratio $\varepsilon = 0.96$ related to the whole valve. The flow is with low velocities. From the isolines of the Mach number, shown on the Fig. 7, it is visible that the highest values of velocity are reached at the throat (min. diameter) of the diffuser $M_{max} = 0.45$. At the flow inlet in the diffuser is the velocity relatively uniform, inside of the diffuser exists the velocity field with a maximum away from the diffuser axis.

The axial component of aerodynamic force at the valve movable part acts in the flow direction, but is very small.

Fig. 8 indicates the distribution of the velocity vectors in the flow field. There are obvious small regions with vortices at the bottom of the main and balancing cones and also in the inner space of the main cone.

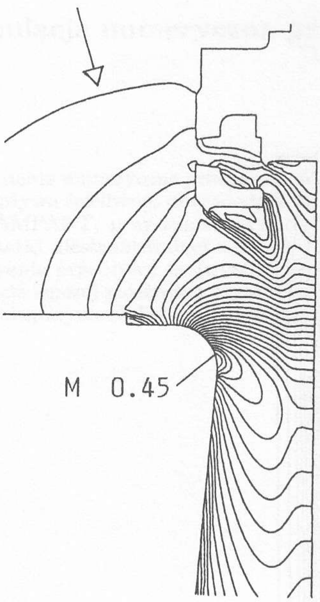

Fig. 7. Isolines of the Mach number for the opened valve $h/D = 0.6$ variant **B**.

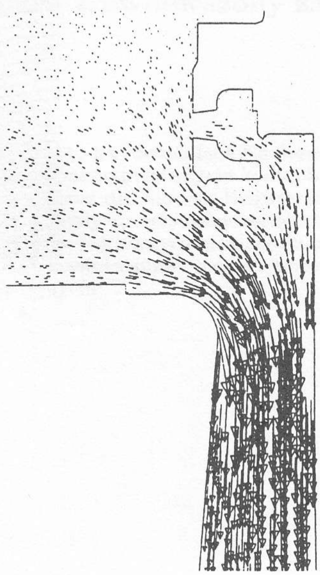

Fig. 8. Velocity vectors distribution for the opened valve $h/D = 0.6$ variant **B**.

The streamlines in the Fig. 9 indicate the uniform flow through the valve. The relative flow through the channel under the main cone amounts to 93%.

3.3. Comparison of the computational and experimental results

Experiments were made with the balanced valve executed according to the Fig. 1. The experiments were made in the air and also in the steam tunnel.

The comparison of experimental results for both variants gives the same results as the calculation.

The mass flow of the variant **B** is greater by 6.5% than that of the variant **A**. The axis component of the aerodynamic force is on the contrary lower for variant **B** by 4,5%.

The experiments proved, that the execution of the balanced valve according to the variant **B** gives more stable flow, with lower excitation forces, what has the effect in the lower vibrations. In Table 1 are compared the values of acceleration a [ms^{-2}], which were measured on stems of the model valves for both variants.

4. Conclusions

From performed work there stem the following conclusions:

- verified was the possibility of the 2D and 3D computation of the flow of compressible, viscous steam through the control valve with good results

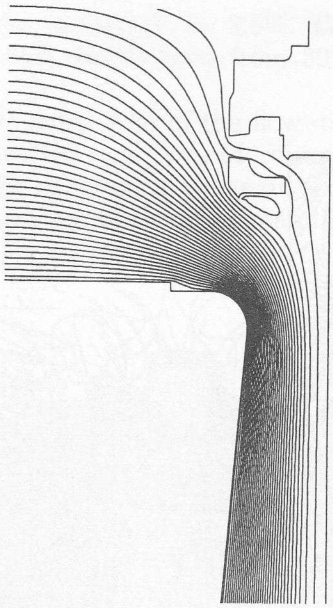

Fig. 9. Streamlines for the opened valve $h/D = 0.6$ variant **B**.

Table 1. Acceleration **a** ms^{-2} on the stem of the model valve

Variant h/D	0.04	0.6
A	10	2.5
B	6	0.5

- the comparison of two variants of the geometry of the main and balancing cones proved the significant difference in the structure of the flow, especially by the small lifts of the main cone
- the variant **B** with the modified shape renders better aerodynamic properties and the calculated improvements agree with the experiments
- experimentally measured vibrations have shown, that the modified valve according to the variant **B** is also more stable due to the lower aerodynamic excitation forces.

Acknowledgement The authors are grateful for the support that was given by the Grant Agency of the Czech Republic under Grant No. 101/96/0054.

Manuscript received in April 1998

Symulacja numeryczna przepływu pary przez zrównoważony zawór regulacyjny

Streszczenie

Obliczenia numeryczne przepływu przez zawór zrównoważony oparto na równaniach Naviera-Stokesa dla przepływu ściśliwego oraz modelu turbulencji k-ε. Obliczenia wykonano przy użyciu kodu obliczeniowego RAMPANT, przy założeniu przepływu osiowo-symetrycznego oraz dla modelu trójwymiarowego. Użyto siatki niestrukturalnej o liczbie (12-8)×103 trójkątów dla przepływu osiowo-symetrycznego. Do modelowania przepływu trójwymiarowego użyto siatki 160 × 106 czworościennych elementów, a w celu osiągnięcia lepszej zbieżności użyto solwera Multigrid. Wyniki modelowania numerycznego porównano z danymi eksperymentalnymi dla zrównoważonych zaworów regulacyjnych.